JACS
JOURNAL OF THE AMERICAN CHEMICAL SOCIETY
Communication
pubs.acs.org/JACS

High Field Solid-State NMR Spectroscopy Investigation of ^{15}N-Labeled Rosette Nanotubes: Hydrogen Bond Network and Channel-Bound Water

Hicham Fenniri,[*,#,‡,†] Grigory A. Tikhomirov,[‡,†] Darren H. Brouwer,[§] Souhaila Bouatra,[‡,†] Mounir El Bakkari,[‡,†] Zhimin Yan,[†] Jae-Young Cho,[†] and Takeshi Yamazaki[†]

[#]313 Snell Engineering Center, Northeastern University, 360 Huntington Avenue, Boston, Massachusetts 02115, United States
[‡]Department of Chemistry and [†]National Institute for Nanotechnology (NINT-NRC), University of Alberta, 11421 Saskatchewan Drive, Edmonton, Alberta T6G 2M9, Canada
[§]Department of Chemistry, Redeemer University College, 777 Garner Road East, Ancaster, Ontario L9K 1J4, Canada

Supporting Information

ABSTRACT: ^{15}N-labeled rosette nanotubes were synthesized and investigated using high-field solid-state NMR spectroscopy, X-ray diffraction, atomic force microscopy, and electron microscopy. The results established the H-bond network involved in the self-assembly of the nanostructure as well as bound water molecules in the nanotube's channel.

Supramolecular nanoscale assembly is an active area of research aimed at developing nanostructured materials with tunable dimensions and physical properties.[1] In particular, self-assembly and self-organization processes are growing into powerful strategies for the generation of a broad range of nanomaterials with applications in medicine,[2] renewable energy,[3] nanoelectronics,[4] and theranostics.[5]

In this context, our group has established a hierarchical self-assembly strategy to produce well-defined nanotubular architectures with tunable dimensions and chemical, physical, and biological properties. The G∧C motifs are synthetic organic DNA base analogues with the hydrogen bonding arrays of both guanine and cytosine (Figure 1A, **1**).[6] Owing to their self-complementary hydrogen bonding arrays and molecular design, the G∧C molecules self-assemble to form rosettes (six-membered supermacrocycle, Figure 1B), which in turn undergo self-assembly into a tubular stack, the rosette nanotubes (RNTs) (Figure 1D).[6a,b,7] These materials have shown unusual optical,[8] chiroptical,[9] and biomedical[10] properties in solution as well as excellent thermal stability (e.g., boiling water)[11] and mechanical resilience under shear force,[12] which motivated our interest in elucidating their H-bonding network.

Although the RNTs have been extensively characterized by electron microscopy, scanning probe microscopy, circular dichroism, UV−vis, dynamic light scattering, and fluorescence spectroscopies,[6−12] their detailed structural characterization at the molecular scale has remained elusive due to the inherent challenges associated with generating suitable single crystals for X-ray diffraction analysis.

Solution-phase nuclear magnetic resonance (NMR) experiments (^{1}H, ^{13}C, ^{15}N NMR; ^{1}H−^{13}C HMQC, ^{1}H−^{13}C HMBC, ^{1}H−^{15}N HSQC, ^{1}H−^{15}N HMQC, ^{1}H−^{15}N gHMBC, NOESY)

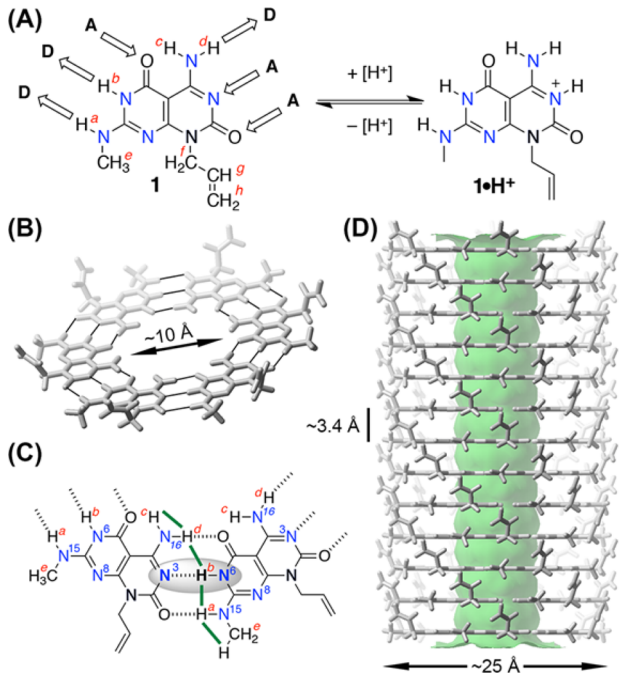

Figure 1. (A) Structures of G∧C base **1** (and its protonated form **1**·**H**$^{+}$) highlighting self-complementary hydrogen bonding pattern (A, acceptor; D, donor; ^{15}N atoms are blue). (B) Molecular model of rosette supermacrocycle formed from the self-assembly of six molecules of **1**. (C) ^{15}N-labeled G∧C derivative **1** highlighting through-space ^{1}H−^{1}H (green lines) and the ^{15}N−^{15}N/^{15}N−^{1}H correlations (grayed area). (D) Molecular model of rosette stack forming a rosette nanotube RNT (**1**).

of the protonated form of the G∧C derivative (**1**·**H**$^{+}$, Figure 1A) revealed the existence of two tautomers in solution (Table S1, Figure S2−S7).[13] **1**·**H**$^{+}$ cannot form RNTs (as it does not feature the correct self-complementary hydrogen bonding code).[6−12] Its neutralization with a base led to extensive line broadening suggesting that the isotropic averaging of the anisotropic nuclear spin interactions by rapid molecular tumbling is significantly

Received: March 6, 2016
Published: May 4, 2016

DOI: 10.1021/jacs.6b02420
J. Am. Chem. Soc. 2016, 138, 6115−6118

hindered upon RNT formation. To overcome this challenge, we turned to solid-state NMR spectroscopy. While solid-state ^{1}H NMR typically suffers from poor spectral resolution (due primarily to the combination of strong ^{1}H−^{1}H dipolar interactions and small ^{1}H chemical shift range), we anticipated that well-resolved NMR spectra of ^{15}N-labeled RNTs could be obtained in a high magnetic field with fast magic-angle spinning (MAS).[14−18]

Herein, we report the synthesis of the first ^{15}N-labeled G∧C base,[13] solid-state NMR experiments performed at an ultrahigh-field magnet field strength (21.1 T), and ultrafast magic angle spinning (MAS) (60 kHz). With this high resolution, we were able to elucidate the spatial arrangement of protons of the G∧C modules by employing a 2D ^{1}H−^{1}H double quantum (DQ) correlation experiment,[14−16] which probes through-space dipolar interactions. Furthermore, we have been able to obtain decisive ^{1}H−^{15}N and ^{15}N−^{15}N 2D correlation spectra, both through-bond and through-space, which provide clear evidence for the hydrogen bonding pattern (Figure 1C) of the self-assembled rosette structure.

The resonances in the ^{1}H (Figure 2A) and ^{15}N (Figure 2B) solid-state NMR spectra can be assigned from the correlation

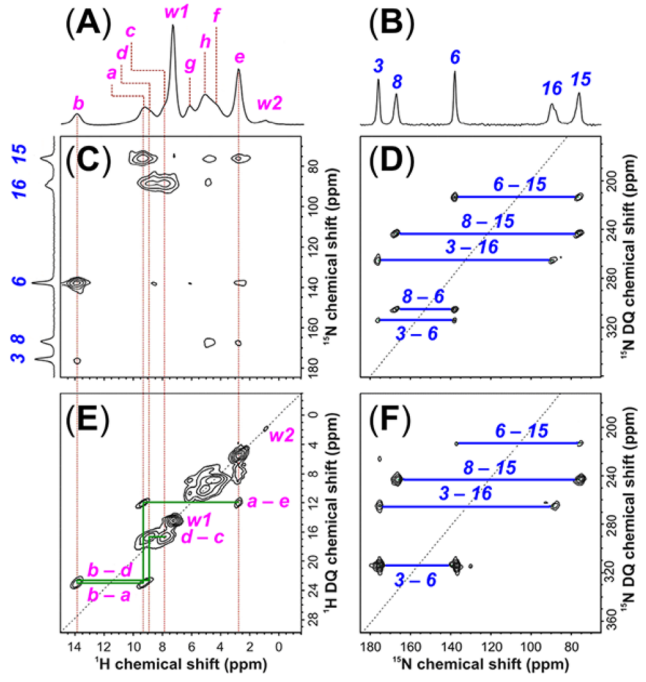

Figure 2. Solid-state NMR spectra of RNT(**1**) acquired at 21.1 T (A, C, E) with 60 kHz MAS frequency and 4.7 T (B, D, F) with 4 kHz MAS frequency: (A) ^{1}H MAS NMR spectrum; (B) ^{15}N CP MAS NMR spectrum; (C) ^{1}H−^{15}N CP HETCOR spectrum (note that this spectrum has been rotated by 90° from the conventional display orientation: ^{15}N was observed in the direct dimension, while ^{1}H was observed in the indirect dimension); (D) ^{15}N−^{15}N SR26$_4$[11] dipolar DQ correlation spectrum;[18] (E) ^{1}H−^{1}H BABA dipolar DQ correlation spectrum;[16] (F) ^{15}N−^{15}N refocused INADEQUATE spectrum.[19−22] Peaks labeled **w** are from water (see text).

peaks observed in the 2D ^{1}H−^{15}N heteronuclear correlation (HETCOR) (Figure 2C) and ^{15}N−^{15}N DQ correlation (Figure 2D) spectra (Table S3),[13] both of which probe through-space dipolar interactions. There are five pieces of evidence in these solid-state NMR spectra that clearly establish the expected hydrogen-bonded molecular arrangement depicted in Figure 1C. First, the observation of NH^{b} proton chemical shift at 13.7 ppm (Figure 2A) suggests N···HN intermolecular hydrogen bonding.[17] Second, the series of correlations in the ^{1}H−^{1}H 2D DQ spectrum involving H^{a}, H^{b}, H^{c}, H^{d}, and H^{e}, indicated by the solid green lines in Figures 1C and 2E, are consistent with the spatial arrangement of these hydrogens, which itself is the result of the self-complementary hydrogen-bonding of the G and C faces of **1**. Third, the ^{1}H−^{15}N 2D HETCOR spectrum (Figure 2C) shows a weak but significant correlation between H^{b} and N$_3$, consistent with the close spatial proximity of H^{b} and N$_3$ that results from the intermolecular N$_3$···H^{b}N$_6$ hydrogen bond. Fourth, the ^{15}N−^{15}N 2D DQ correlation spectrum (Figure 2D) shows a correlation between N$_3$ and N$_6$. Given the spatial arrangement of these nitrogen atoms in compound **1**, the observed dipolar coupling is consistent with an intermolecular interaction resulting from an intermolecular hydrogen bond between N$_3$ and N$_6$, rather than the much farther intramolecular interaction.

Finally, the ^{15}N−^{15}N 2D INADEQUATE spectrum (Figure 2F) correlates pairs of nuclear spins for which there exists a through-bond *J*-coupling. The spectrum shows a very strong correlation between N$_3$ and N$_6$. This correlation can only arise from the existence of an intermolecular hydrogen bond between N$_3$ and N$_6$ in which the hydrogen bond mediates the *J*-coupling between the ^{15}N spin pairs. $^{2h}J_{\mathrm{N-H\cdots N}}$ couplings have previously[19−21] been reported in solid-state supramolecular materials and have even been measured to be in the range of 5.9−7.4 Hz, while the other two-bond ^{15}N−^{15}N *J*-couplings have been measured to be 3.5−6.6 Hz.[20] In summary, these five separate solid-state NMR experiments provided unambiguous evidence for the hydrogen-bonded molecular arrangement of module **1** within rosette **1**$_6$ and RNT(**1**).

The ^{13}C CP-MAS spectrum (Figure S9)[13] supports the RNT structure as it shows severely broadened lineshapes for the allyl peaks, indicating a significant distribution of ^{13}C chemical shifts. This suggests that the allyl groups, on the surface of the RNTs, are disordered over various bonding geometries. These results are consistent with an RNT structure having an ordered core (as seen by sharp peaks) with disordered surface groups.

We have previously investigated the role of water in self-assembly, conformational stability, and chiroptical properties of the RNTs.[9b,c] In particular, we carried out a theoretical analysis of the molecular structure and thermodynamics of solvation both around the RNT and inside its channel using the three-dimensional molecular theory of solvation.[23] This study revealed how water contributes to the stability of the RNTs by mediating effective inter-rosette H-bonds and determines the RNT self-assembly pathway. Notably, two types of water molecules were identified in the inner channel (referred to as w1 and w2). w1 (six molecules per rosette forming a ring-like structure inside the channel) was found to bridge carbonyl groups between consecutive rosette rings with an affinity of 0.64 kcal/mol of water. w2 was confined to the center of the inner channel as a loose chain of water molecules (one molecule per rosette, 0.27 kcal/mol of water).

In agreement with our predictions, we were able to identify two solvent peaks in the proton NMR spectra at 7 and 1 ppm (Figure 2A), which were assigned to the two types of water molecules (w1/w2). Neither of these peaks have correlations to the ^{1}H and ^{15}N nuclei of the G∧C bases, probably because of their dynamic nature. It should be noted that the peak for bulk-like water usually resonates at 4.8 ppm. The remarkable downfield/upfield shifts observed (ca. 2.2/3.8 ppm) suggest a considerable through-space deshielding/shielding effect of the

DOI: 10.1021/jacs.6b02420
J. Am. Chem. Soc. 2016, 138, 6115−6118

RNTs, an effect that has been observed in other supramolecular host–guest systems.[24] They may also be the result of altered hydrogen bond geometries in the confined channel space.[24e]

The well-resolved signals at 13.7 and 7.0/1.0 ppm due to H^b and w1/w2, respectively, offered an opportunity to quantify the number of confined water molecules. Integration of these peaks gave a ratio of 3:6:1 for H^b/w1/w2, which suggests that there are seven water molecules for each rosette ring formed from six G∧C bases, consistent with our modeling studies.[23] The fact that $^1H-^1H$ DQ correlations for the interior water are observed only along the diagonal (Figure 2E) suggests that these molecules have a degree of restrained mobility, lacking the full (isotropic) mobility that would lead to complete averaging of strong dipolar interactions to zero. Their mobility may be sufficiently restrained such that the strong internal dipolar couplings between protons of a single water molecule are not fully averaged, leading to correlations along the diagonal. However, the residual mobility may be sufficient to average the much weaker dipolar couplings to the nuclei of the G∧C units that make up the walls of the nanotube, such that no additional correlations are observed.[25]

Whereas solid-state NMR spectroscopy provided clear local structural information about the hydrogen-bonded molecular arrangement, powder X-ray diffraction (XRD) provided additional information about periodic features of the structure over larger length scales. The powder XRD pattern of RNT(**1**) (Figure 3A) shows a small number of broadened reflections. The

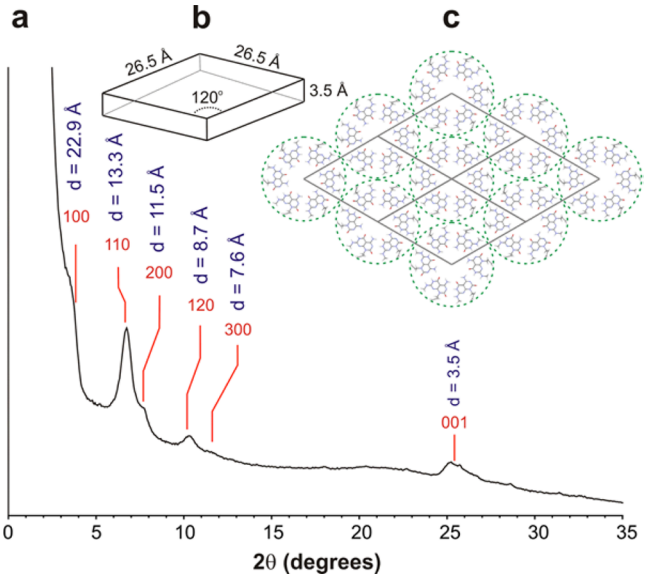

Figure 3. Powder XRD pattern obtained for RNT(**1**) powder (a) indexed according to hexagonal packing model (b,c).

peak near $2\theta = 25°$ (d-spacing of 3.5 Å) likely corresponds to the distance between adjacent rosette units that stack to make up the nanotubes. The remaining small angle reflections are consistent with a hexagonal unit cell having a lattice parameter of 26.5 Å, as depicted in Figure 3B. Based on these observations, we propose a model in which the nanotubes, each having a diameter of approximately 25 Å, bundle into a hexagonal array as depicted in Figure 3C. Hexagonal packing is very common for cylindrical objects such as discotic liquid crystalline phases[26] and carbon nanotubes.[27] Indeed, SEM and TEM of **1** show bundles of RNTs.[13] The fact that the reflections are heavily broadened indicates a distribution of inter-rosette and internanotube distances resulting from imperfect rosette stacking and nanotube packing.

In summary, our earlier reports[6−12] on RNT structure were based on dimensions (TEM, STM, AFM), spectroscopy (FTIR, 1D/2D $^1H/^{13}C$ NMR, UV−vis, CD), and computational studies but no experimental evidence was available to unambiguously assign the H-bond network to a stack of rosettes rather than a helix, double helix, or a tape. Particularly, it is very unusual for a small organic molecule such as **1** to form such an elaborate and stable architecture (RNT), in water, through H-bonds. This report presents the first conclusive evidence for the hydrogen bonding pattern of RNTs assembled from G∧C modules and establishes the relevance and importance of high-field solid state NMR for the investigation of supramolecular nanoscale systems that are not amenable to single crystal X-ray analysis. Furthermore, these results substantiate our earlier predictions of the dual role of water as the principal source of energy for self-assembly (hydrophobic effect)[7,23] and as structural water (by stitching the G∧C bases in the channel).[23] Future studies will aim to investigate the transport properties of the RNTs and hence the dynamics of w1/w2 in the channel using variable-temperature solid state NMR exchange spectroscopy, infrared spectroscopy, and H/D exchange experiments.[28]

■ ASSOCIATED CONTENT

Supporting Information

The Supporting Information is available free of charge on the ACS Publications website at DOI: 10.1021/jacs.6b02420.

Synthesis and characterization of **1**, SEM and TEM of **1**, RNT sample preparation, solution state NMR of **1**·H^+, solution state characterization of G∧C bases to elucidate structure and resolve 2D NMR assignments, solid state NMR details, and PXRD details (PDF)

■ AUTHOR INFORMATION

Corresponding Author

*h.fenniri@neu.edu

Present Addresses

(G.T.) Division of Biology and Biological Engineering, California Institute of Technology, 1200 East California Boulevard, Pasadena, California 91125, United States.

(T.Y.) Vancouver Prostate Centre, 2660 Oak Street, Vancouver, BC V6H 3Z6, Canada.

(S.B.) Department of Biological Sciences, University of Alberta, Edmonton, AB 26G 2E8, Canada.

Notes

The authors declare no competing financial interest.

■ ACKNOWLEDGMENTS

Access to the 900 MHz NMR spectrometer was provided by the National Ultrahigh Field NMR Facility for Solids, a national research facility funded by the Canada Foundation for Innovation, the Natural Sciences and Engineering Research Council of Canada (NSERC), the Ontario Innovation Trust, Recherche Québec, the National Research Council Canada (NRC), and Bruker BioSpin and managed by the University of Ottawa. We thank NSERC, NRC, the University of Alberta, and Northeastern University for financial support.

■ REFERENCES

(1) (a) Kim, Y.; Macfarlane, R. J.; Jones, M. R.; Mirkin, C. A. *Science* **2016**, *351*, 579–582. (b) Douglas, S. M.; Dietz, H.; Liedl, T.; Högberg,

DOI: 10.1021/jacs.6b02420
J. Am. Chem. Soc. 2016, 138, 6115–6118

B.; Graf, F.; Shih, W. M. *Nature* **2009**, *459*, 414−418. (c) Zhang, F.; Nangreave, J.; Liu, Y.; Yan, H. *J. Am. Chem. Soc.* **2014**, *136*, 11198−11211.
(2) (a) Chao, J.; Liu, H.; Su, S.; Wang, L.; Huang, W.; Fan, C. *Small* **2014**, *10*, 4626−4635. (b) Shi, J.; Xiao, Z.; Kamaly, N.; Farokhzad, O. C. *Acc. Chem. Res.* **2011**, *44*, 1123−1134.
(3) (a) Lu, L.; Zheng, T.; Wu, Q.; Schneider, A. M.; Zhao, D.; Yu, L. *Chem. Rev.* **2015**, *115*, 12666−12731. (b) Peng, H.-Q.; Niu, L.-Y.; Chen, Y.-Z.; Wu, L.-Z.; Tung, C.-H.; Yang, Q.-Z. *Chem. Rev.* **2015**, *115*, 7502−7542.
(4) (a) Chen, S.; Slattum, P.; Wang, C.; Zang, L. *Chem. Rev.* **2015**, *115*, 11967−11998. (b) Mallia, A. R.; Salini, P. S.; Hariharan, M. *J. Am. Chem. Soc.* **2015**, *137*, 15604−15607. (c) Dou, L.; Liu, Y.; Hong, Z.; Li, G.; Yang, Y. *Chem. Rev.* **2015**, *115*, 12633−12665.
(5) (a) Zhou, W.; Gao, X.; Liu, D.; Chen, X. *Chem. Rev.* **2015**, *115*, 10575−10636. (b) Aznar, E.; Oroval, M.; Pascual, L.; Murguía, J. R.; Martínez-Máñez, R.; Sancenón, F. *Chem. Rev.* **2016**, *116*, 561−718. (c) Zhang, A.; Lieber, C. M. *Chem. Rev.* **2016**, *116*, 215−257.
(6) (a) Fenniri, H.; Packiarajan, M.; Vidale, K. L.; Sherman, D. M.; Hallenga, K.; Wood, K. V.; Stowell, J. G. *J. Am. Chem. Soc.* **2001**, *123*, 3854−3855. (b) Durmus, A.; Gunbas, G.; Farmer, S. C.; Olmstead, M. M.; Mascal, M.; Legesse, B.; Cho, J.-Y.; Beingessner, R. B.; Yamazaki, Takeshi; Fenniri, H. *J. Org. Chem.* **2013**, *78*, 11421−11426. (c) Marsh, A.; Silvestri, M.; Lehn, J.-M. *Chem. Commun.* **1996**, 1527−1528. (d) Kolotuchin, S. V.; Zimmerman, S. C. *J. Am. Chem. Soc.* **1998**, *120*, 9092−9093.
(7) (a) Fenniri, H.; Deng, B. L.; Ribbe, A. E.; Hallenga, K.; Jacob, J.; Thiyagarajan, P. *Proc. Natl. Acad. Sci. U. S. A.* **2002**, *99*, 6487−6492. (b) Chhabra, R.; Moralez, J. G.; Raez, J.; Yamazaki, T.; Cho, J.-Y.; Myles, A. J.; Kovalenko, A.; Fenniri, H. *J. Am. Chem. Soc.* **2010**, *132*, 32−33.
(8) Borzsonyi, G.; Beingessner, R. L.; Yamazaki, T.; Cho, J.-Y.; Myles, A. J.; Malac, M.; Egerton, R.; Kawasaki, M.; Ishizuka, K.; Kovalenko, A.; Fenniri, H. *J. Am. Chem. Soc.* **2010**, *132*, 15136−15139.
(9) (a) Fenniri, H.; Deng, B. L.; Ribbe, A. E. *J. Am. Chem. Soc.* **2002**, *124*, 11064−11072. (b) Johnson, R. S.; Yamazaki, T.; Kovalenko, A.; Fenniri, H. *J. Am. Chem. Soc.* **2007**, *129*, 5735−5743. (c) Hemraz, U. D.; El Bakkari, M.; Yamazaki, T.; Cho, J.-Y.; Beingessner, R. L.; Fenniri, H. *Nanoscale* **2014**, *6*, 9421−9427.
(10) (a) Childs, A.; Hemraz, U. D.; Castro, N. J.; Fenniri, H.; Zhang, L. G. *Biomed. Mater.* **2013**, *8*, 065003. (b) Ong, K. J.; MacCormack, T. J.; Clark, R. J.; Ede, J. D.; Felix, L.; Ortega, V.; Dang, M. K. M.; Ma, G.; Fenniri, H.; Veinot, J. G. C.; Goss, G. G. *PLoS One* **2014**, *9*, e90650. (c) Chun, A. L.; Moralez, J. G.; Webster, T. J.; Fenniri, H. *Biomaterials* **2005**, *26*, 7304−7309. (d) Singh, S. S.; Rakotondradany, F.; Myles, A. J.; Fenniri, H.; Singh, B. *Biomaterials* **2009**, *30*, 3084−3090.
(11) Moralez, J. G.; Raez, J.; Yamazaki, T.; Motkuri, R. K.; Kovalenko, A.; Fenniri, H. *J. Am. Chem. Soc.* **2005**, *127*, 8307−8309.
(12) Raez, J.; Moralez, J. G.; Fenniri, H. *J. Am. Chem. Soc.* **2004**, *126*, 16298−16299.
(13) See Supporting Information.
(14) Brown, S. P.; Spiess, H. W. *Chem. Rev.* **2001**, *101*, 4125−4155.
(15) Schnell, I.; Spiess, H. W. *J. Magn. Reson.* **2001**, *151*, 153−227.
(16) (a) Schnell, I. *Prog. Nucl. Magn. Reson. Spectrosc.* **2004**, *45*, 145−207. (b) Brown, S. P. *Prog. Nucl. Magn. Reson. Spectrosc.* **2007**, *50*, 199−251.
(17) Webber, A. L.; Masiero, S.; Pieraccini, S.; Burley, J. C.; Tatton, A. S.; Iuga, D.; Pham, T.; Spada, G. P.; Brown, S. P. *J. Am. Chem. Soc.* **2011**, *133*, 19777−19795.
(18) Kristiansen, P. E.; Carravetta, M.; Lai, W. C.; Levitt, M. H. *Chem. Phys. Lett.* **2004**, *390*, 1−7.
(19) Pham, T. N.; Griffin, J. M.; Masiero, S.; Lena, S.; Gottarelli, G.; Hodgkinson, P.; Fillip, C.; Brown, S. P. *Phys. Chem. Chem. Phys.* **2007**, *9*, 3416−3423.
(20) Pham, T. N.; Masiero, S.; Gottarelli, G.; Brown, S. P. *J. Am. Chem. Soc.* **2005**, *127*, 16018−16019.
(21) Brown, S. P.; Perez-Torralba, M.; Sanz, D.; Claramunt, R. M.; Emsley, L. *J. Am. Chem. Soc.* **2002**, *124*, 1152−1153.
(22) Lesage, A.; Bardet, M.; Emsley, L. *J. Am. Chem. Soc.* **1999**, *121*, 10987.
(23) Yamazaki, T.; Fenniri, H.; Kovalenko, A. *ChemPhysChem* **2010**, *11*, 361−367.
(24) (a) Chen, Q.; Herberg, J. L.; Mogilevsky, G.; Wang, H.; Stadermann, M.; Holt, J. K.; Wu, Y. *Nano Lett.* **2008**, *8*, 1902−1905. (b) Brunklaus, G.; Koch, A.; Sebastiani, D.; Spiess, H. W. *Phys. Chem. Chem. Phys.* **2007**, *9*, 4545−4551. (c) Kurotobi, K.; Murata, Y. *Science* **2011**, *333*, 613−616. (d) Brouwer, D. H.; Alavi, S.; Ripmeester, J. A. *Phys. Chem. Chem. Phys.* **2008**, *10*, 3857−3860. (e) Limbach, H.-H; Tolstoy, P. M.; Pérez -Hernández, N.; Guo, J.; Shenderovich, I. G.; Denisov, G. S. *Isr. J. Chem.* **2009**, *49*, 199−216.
(25) Hoffmann, A.; Sebastiani, D.; Sugiono, E.; Yun, S.; Kim, K. S.; Spiess, H. W.; Schnell, I. *Chem. Phys. Lett.* **2004**, *388*, 164−169.
(26) Ziessel, R.; Pickaert, G.; Camerel, F.; Donnio, B.; Guillon, D.; Cesario, M.; Prange, T. *J. Am. Chem. Soc.* **2004**, *126*, 12403−12413.
(27) Colomer, J. F.; Henrard, L.; Flahaut, E.; Van Tendeloo, G.; Lucas, A. A.; Lambin, P. *Nano Lett.* **2003**, *3*, 685−689.
(28) (a) Febles, M.; Pérez-Hernández, N.; Pérez, C.; Rodríguez, M. L.; Foces-Foces, C.; Roux, M. V.; Morales, E. Q.; Buntkowsky, G.; Limbach, H.-H.; Martín, J. D. *J. Am. Chem. Soc.* **2006**, *128*, 10008−10009. (b) Pérez-Hernández, N.; Luong, T. Q.; Febles, M.; Marco, C.; Limbach, H.-H.; Havenith, M.; Pérez, C.; Roux, M. V.; Pérez, R.; Martín, J. D. *J. Phys. Chem. C* **2012**, *116*, 9616−9630.

DOI: 10.1021/jacs.6b02420
J. Am. Chem. Soc. 2016, 138, 6115−6118